Charm-Quark Production in Deep-Inelastic Neutrino Scattering at Next-to-Next-to-Leading Order in QCD

Edmond L. Berger,[1,*] Jun Gao,[1,†] Chong Sheng Li,[2,3,‡] Ze Long Liu,[2,§] and Hua Xing Zhu[4,‖]
[1]*High Energy Physics Division, Argonne National Laboratory, Argonne, Illinois 60439, USA*
[2]*Department of Physics and State Key Laboratory of Nuclear Physics and Technology, Peking University, Beijing 100871, China*
[3]*Center for High Energy Physics, Peking University, Beijing 100871, China*
[4]*Center for Theoretical Physics, Massachusetts Institute of Technology, Cambridge, Massachusetts 02139, USA*
(Received 26 January 2016; revised manuscript received 1 April 2016; published 24 May 2016)

We present a fully differential next-to-next-to-leading order calculation of charm-quark production in charged-current deep-inelastic scattering, with full charm-quark mass dependence. The next-to-next-to-leading order corrections in perturbative quantum chromodynamics are found to be comparable in size to the next-to-leading order corrections in certain kinematic regions. We compare our predictions with data on dimuon production in (anti)neutrino scattering from a heavy nucleus. Our results can be used to improve the extraction of the parton distribution function of a strange quark in the nucleon.

DOI: 10.1103/PhysRevLett.116.212002

Introduction.—Charm-quark (c) production in deep-inelastic scattering (DIS) of a neutrino from a heavy nucleus provides direct access to the strange-quark (s) content of the nucleon. At lowest order, the relevant partonic process is neutrino interaction with a strange quark, $\nu s \to cl$, mediated by weak vector boson W exchange. Another source of constraints is charm-quark production in association with a W boson at hadron colliders, $gs \to cW$. The DIS data determine parton distribution functions (PDFs) in the nucleon whose detailed understanding is vital for precise predictions at the Large Hadron Collider (LHC). The strange-quark PDF can play an important role in LHC phenomenology, contributing, for example, to the total PDF uncertainty in W or Z boson production [1,2], and to systematic uncertainties in precise measurements of the W boson mass and weak-mixing angle [3–5]. It is estimated that the PDF uncertainty of the strange quark alone could lead to an uncertainty of about 10 MeV on the W boson mass measurement at the LHC [6]. From the theoretical point of view, it is important to test whether the strange PDFs are suppressed compared to those of other light sea quarks, related to the larger mass of the strange quark, as suggested by various models [7–9], and to establish whether there is a difference between the strange- and antistrange-quark PDFs.

In this Letter, we report on a complete calculation at next-to-next-to-leading order (NNLO) in pertubative quantum chromodynamics (QCD) of charm-quark production in DIS of a neutrino from a nucleon. Our calculation is based on a phase-space slicing method and uses a fully differential Monte Carlo integration. It maintains the exact mass dependence and all kinematic information at the parton level. The NNLO corrections can change the cross sections by up to 10%, depending on the kinematic region considered. Our results show that the next-to-leading-order (NLO) predictions underestimate the perturbative uncertainties owing to accidental cancellations at that order. Our calculation is an important ingredient for future global analyses of PDFs at NNLO in QCD, especially for extracting the strange quark PDFs. The results can also be used to correct for acceptance in experimental analyses. In this Letter, we show comparisons of our results with data from the NuTeV and NOMAD collaborations [10,11], indicating that, once the NNLO corrections are included, slightly higher strangeness PDFs are preferred in the low-x region than those based on a NLO analysis.

Ours is the first complete NNLO calculation of QCD corrections to charm-quark production in weak charged-current deep-inelastic scattering. In all current analyses which include charm-quark production data in neutrino DIS, the hard-scattering cross sections are calculated only at NLO [12–14], without including an estimation of the remaining higher-order perturbative uncertainties. Approximate NNLO [15] results are available for a very large momentum transfer. However, for neutrino DIS experiments [10,11,16,17], the typical momentum transfer is small and the exact charm-quark mass dependence must be kept [15,18]. Recently, $O(\alpha_s^3)$ results [19] became available for structure function xF_3 at large momentum transfer.

In the Letter, we outline the method used in the calculation, present our numerical results showing their stability under parameter variation, and then compare our results with data in the kinematic regions of the experimental acceptance.

Method.—The process of interest is the production of a charm quark in DIS, $\nu_\mu(p_{\nu_\mu}) + N(p_N) \to \mu^-(p_{\mu^-}) + c(p_c) + X(p_X)$, where X represents the final hadronic state, excluding the charm quark. We work in the region where the momentum transfer $Q^2 = -q^2 = -(p_{\nu_\mu} - p_{\mu^-})^2$ is much larger than the perturbative scale, $\Lambda^2_{\rm QCD}$, and perturbative QCD can be trusted. The calculation of

QCD corrections beyond LO requires a proper handling of divergences in loop and phase-space integrals which must be canceled consistently to produce physical results. Methods based on subtraction [20,21] or phase-space slicing [22] have been shown to be successful at NLO. The NNLO case is less well developed, although several methods have been proposed [23–29]. For this calculation, we employ phase-space slicing at NNLO [30], which is a generalization of the q_T-subtraction concept of Catani and Grazzini [25]. Specifically, we use the N-jettiness variable of Stewart, Tackmann, and Waalewijn [31] to divide the final state at NNLO into resolved and unresolved regions. Phase-space slicing based on this observable is also dubbed the N-jettiness subtraction. For recent applications of N-jettiness subtraction, see Refs. [32,33]. We define

$$\tau = \frac{2p_X \cdot p_n}{Q^2 + m_c^2}, \qquad p_n = (\bar{n} \cdot (p_c - q))\frac{n^\mu}{2}, \tag{1}$$

where m_c denotes the charm-quark mass, $n = (1, 0, 0, 1)$ specifies the direction of the incoming hadron in the center of mass frame, and $\bar{n} = (1, 0, 0, -1)$ denotes the opposite direction. Following Ref. [34], we call τ 0-jettiness in this Letter. We refer to the region $\tau \ll 1$ as unresolved and the region $\tau \sim 1$ as resolved. We discuss the calculation of the cross section in these two regions separately.

In the unresolved region, $p_X \cdot p_n \sim 0$, i.e., p_X consists of either soft partons, hard partons collinear to an incoming hadron, or both. Using the machinery of soft-collinear effective theory (SCET) [35–38], one may show that the cross section in this region obeys a factorization (fact.) theorem [39,40]:

$$\frac{d\sigma_{\rm fact}}{d\tau} = \int_0^1 dz \hat{\sigma}_0(z) |C(Q, m_c, \mu)|^2 \int d\tau_n d\tau_s \times \delta(\tau - \tau_n - \tau_s) B_q(\tau_n, z, \mu) S(\tau_s, n \cdot v, \mu), \tag{2}$$

where $\hat{\sigma}_0(z)$ is the LO partonic cross section for the reaction $s(zp_N) + \nu_\mu(p_{\nu_\mu}) \to c(p_c) + \mu^-(p_{\mu^-})$. $C(Q, m_c, \mu) = 1 + O(\alpha_s)$ is the hard Wilson coefficient obtained from matching QCD to SCET. It encodes all of the short distance corrections to the reaction. Collinear radiation and soft radiation are described by the beam $B_q(\tau_n, z, \mu)$ and soft functions $S(\tau_s, n \cdot v, \mu)$. At LO, they have the simple form

$$B_q(\tau_n, z, \mu) = \delta(\tau_n) f_{s/N}(z, \mu), \qquad S(\tau_s, n \cdot v, \mu) = \delta(\tau_s),$$

where $f_{s/N}(z, \mu)$ is the PDF.

The factorization formula equation (2) provides a simplified description of the cross section, fully differential in the leptonic part and the heavy quark part, and correct up to power corrections in τ. The 0-jettiness parameter τ controls the distance away from the strictly unresolved region, $\tau = 0$. In fixed order perturbation theory, $d\sigma/d\tau$ diverges as $\alpha_s^k \ln^{2k-1} \tau/\tau$, as a result of an incomplete cancellation of virtual and real contributions. The strength of the SCET approach to describing the unresolved region is that each individual component in the factorization formula equation (2) has its own operator definition and can be computed separately.

All of the ingredients required in this Letter have been computed through two loops for different purposes. Specifically, the hard Wilson coefficient can be obtained by crossing the corresponding hard Wilson coefficient calculated for a $b \to uW^-$ decay [41–44]. The two-loop soft function and beam function were calculated in Refs. [45,46]. After substituting the two-loop expressions for the individual components into Eq. (2), we obtain the desired two-loop expansion of the cross section in the unresolved region [40].

In the resolved region, besides the beam jet, there is at least one additional hard jet with large recoil against the beam. While we do not have a factorization formula in this region, the soft and collinear singularities are relatively simple. Owing to the presence of the hard recoil jet, there is at most one parton which can become soft or collinear. A singularity of this sort can be handled by the standard methods used at NLO. The relevant ingredients are (a) one-loop amplitudes for charm plus one jet production which we take from [47] and cross-check with GOSAM [48], (b) the tree-level amplitudes for charm plus two jet production [49], and (c) NLO dipole subtraction terms [50] for canceling infrared singularities between one-loop and tree-level matrix elements.

After introducing an unphysical cutoff parameter δ_τ, we combine the contributions from the two phase-space regions,

$$\sigma = \int_0^{\delta_\tau} \frac{d\sigma_{\rm fact}}{d\tau} + \int_{\delta_\tau}^{\tau_{\rm max}} \frac{d\sigma}{d\tau} + O(\delta_\tau). \tag{3}$$

Power corrections in δ_τ come from the use of a factorization formula in the unresolved region. In order to suppress the power corrections, a small value of δ_τ is required. On the other hand, the integrations in both the unresolved and resolved regions produce large logarithms of the form $\alpha_s^k \ln^{2k} \delta_\tau$ at $\mathrm{N^kLO}$. The integral over τ can be done analytically in the unresolved region. In the resolved region, the large logarithms of $\ln \delta_\tau$ result from numerical integration near the singular boundary of phase space, resulting in potential numerical instability. A balance has to be reached between suppressing power corrections in δ_τ and reducing numerical instability.

Numerical results.—We first present our numerical results for the total cross section. We use CT14 NNLO PDFs [51] with $N_l = 3$ active quark flavors and the associated strong coupling constant. We use a pole mass $m_c = 1.4$ GeV for the charm quark, and the Cabibbo-Kobayashi-Maskawa (CKM) matrix elements $|V_{cs}| = 0.975$ and $|V_{cd}| = 0.222$ [52]. The renormalization scale is set to $\mu_0 = \sqrt{Q^2 + m_c^2}$ unless otherwise specified. In Fig. 1, we plot the NNLO corrections to the reduced cross section [16] of charm-quark production in DIS of a neutrino on iron, as a function of the phase-space cutoff parameter δ_τ [53].

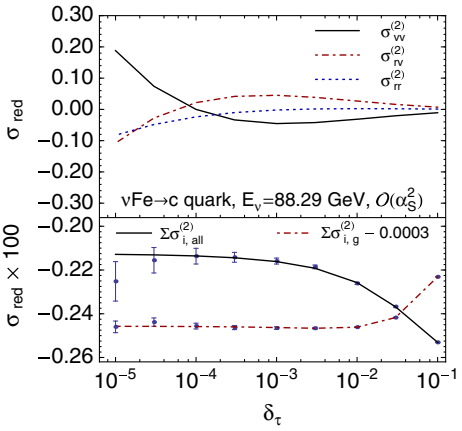

FIG. 1. Dependence of various components of the $O(\alpha_s^2)$ reduced cross sections on the cutoff parameter for charm-quark production in neutrino DIS from iron. (Upper panel) Double-virtual (VV), real-virtual (RV), and double-real (RR) contributions to the full $O(\alpha_s^2)$ corrections. (Lower panel) The full correction (solid line) and the contribution from the gluon channel shifted by a constant.

In the upper panel of Fig. 1 we show three separate contributions to the NNLO corrections: the double-virtual part (VV) contributing to the below cutoff region, and the real-virtual (RV) and double-real (RR) parts contributing to the above cutoff region. Although the individual contributions vary considerably with δ_τ, the total contribution is rather stable and approaches the true NNLO correction when δ_τ is small. The cancellation of the three pieces is about one out of a hundred. In the lower panel of Fig. 1, we show the full NNLO correction as well as its dominant contribution from the gluon channel. Corrections from production initiated by the strange quark or down quark through off-diagonal CKM matrix elements—and all other quark flavors—are small compared to the gluon channel. The error bars indicate the statistical errors from MC integration and the smooth line is a least-χ^2 fit of the dependence of the correction on δ_τ. As expected, the correction is insensitive to the cutoff when δ_τ is small. We find optimal values of δ_τ of approximately $10^{-4} \sim 10^{-3}$, for which the power corrections are negligible while preserving MC integration stability. According to our fitted results, the remaining power corrections there are estimated to be only a few percent of the NNLO correction itself.

In neutrino DIS experiments, differential cross sections are presented in terms of the Bjorken variable x or the inelasticity y. We examined the NLO and NNLO QCD corrections to the differential cross section in x for neutrino scattering on iron, observing that the NNLO corrections are comparable to the NLO corrections in the low-x region. When computing the LO, NLO, and NNLO cross sections throughout this Letter, we consistently use the same NNLO CT14 PDFs [51] in order to focus on effects from the matrix elements at the different orders. Decomposing the full corrections into different partonic channels, we found that the perturbative convergence is well maintained at NNLO for gluon or quark channels individually [40]. The NNLO correction to the quark channel is much smaller than at NLO, and the NNLO correction to the gluon channel is also below half of the NLO correction. However, at NLO there is a large cancellation between the gluon and quark channels in the small x region. We regard this cancellation as *accidental* in that it does not arise from basic principles but is a result of several factors. A similar cancellation has also been observed in the calculation for t-channel single top quark production [54].

In Fig. 2, we display the scale variation envelope of the LO, NLO, and NNLO calculations for the differential distribution in x, normalized to the LO prediction with a nominal scale choice. The bands are calculated by varying the renormalization and factorization scales together, $\mu_R = \mu_F = \mu$, up and down by a factor of 2 around the nominal scale μ_0, avoiding going below the charm-quark mass. At a low x, the NLO scale variations underestimate the perturbative uncertainties owing to the accidental cancellations mentioned in the previous paragraph. The NLO scale variations do not reflect the size of the cancellations between different partonic channels. The NNLO scale variations give a more reliable estimation of the perturbative uncertainties and also show improvement at high x compared with the NLO case.

Comparisons with data.—We turn to an examination of the effects of the NNLO corrections in the kinematic regions of two specific neutrino DIS experiments. The first is the NuTeV Collaboration measurement of charm-(anti)quark production from (anti)neutrino scattering from iron [10,16]. They measure the cross sections for dimuon final states, where one of the muons arises from the primary interaction vertex and the other one from the semileptonic decay of the produced charmed hadron. Kinematic acceptance and the inclusive branching ratio to a muon are applied to convert the dimuon cross sections to cross sections of charm-(anti)quark production at the parton level. These dimuon data from

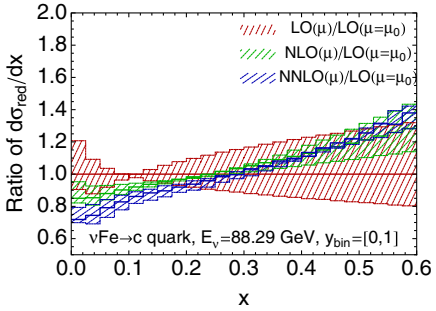

FIG. 2. Scale variations at LO, NLO, and NNLO of the differential distribution in x for charm-quark production in neutrino DIS from iron, normalized to the LO distribution with the nominal scale choice. The solid line shows the corresponding central prediction with the nominal scale choice.

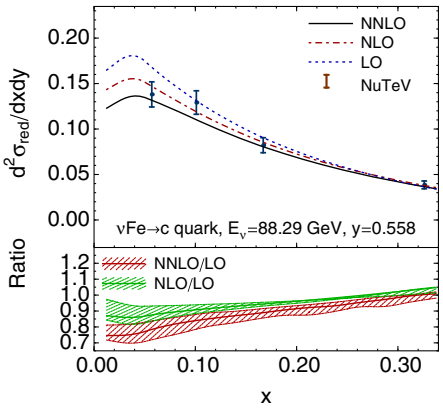

FIG. 3. Comparison of theoretical predictions to the doubly differential cross sections measured by NuTeV for charm-quark production through neutrino DIS from iron.

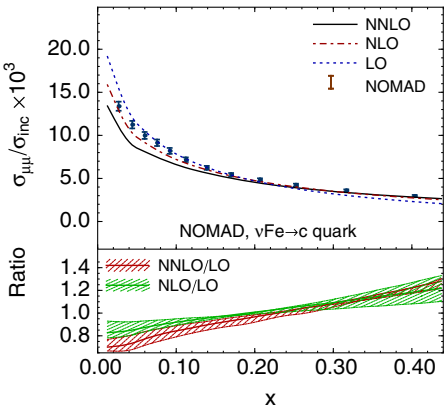

FIG. 4. Comparison of theoretical predictions for ratios of the dimuon cross section to the inclusive charged-current cross section measured by NOMAD for neutrino DIS from iron.

NuTeV have been included in most of the NNLO fits of PDFs and have played an important role in constraining strangeness PDFs. The data are presented as doubly differential cross sections in x and y. In Fig. 3 we show a comparison of theoretical predictions with the data for neutrino scattering with $y = 0.558$, for several values of x. As expected, the NLO calculations generally agree with the data since the same data and the same NLO theoretical expressions are used in the CT14 global analyses [51]. The NNLO corrections are negative in the region of the data and can be as large as 10% of the NLO predictions, as shown in the lower panel of Fig. 3. Based on this comparison, we expect that once the NNLO corrections are included in the global analysis fits, the preferred central values of strange-quark PDFs will be shifted upward. The shift represents one of the theoretical systematics that has not yet been taken into account in any of the current global analyses.

The second set of data is from the NOMAD Collaboration measurement of neutrino scattering from iron [11]. They present ratios of dimuon cross sections to inclusive charged-current cross sections $\mathcal{R}_{\mu\mu} \equiv \sigma_{\mu\mu}/\sigma_{\rm inc}$ instead of converting the dimuon cross sections back to charm-quark production. The measurement is done with a neutrino beam of continuous energy that peaks at approximately 20 GeV. A Q^2 cut of 1 GeV^2 has been applied. In Fig. 4 we show our comparisons of predictions to data as a function of x. Here, we consistently use the NNLO results for $\sigma_{\rm inc}$ in the denominator of the ratio, obtained from the program OPENQCDRAD [55,56]. By LO, NLO, and NNLO, in the figure we refer to our calculations of the dimuon cross sections in the numerator of the ratio. The NLO calculations generally agree with the data, although these data are not included in the CT14 global analyses. The NNLO corrections are negative and can reach about 10% of the LO cross sections in the low-x region covered by the data. At a high x, the NNLO corrections are only a few percent and become positive. The NNLO corrections in Fig. 4 are generally larger than the experimental errors. Thus, they can be very important for extracting strange-quark PDFs in analyses with NOMAD data included. We also plot the scale variation bands in the lower panel of Fig. 4. The trends are similar to the ones in Fig. 2. The NLO predictions underestimate the perturbative uncertainty. It can still reach $\pm 5\%$ at NNLO in the low-x region and can be reduced once even higher-order corrections are included.

Summary.—We present the first complete calculation of NNLO QCD corrections to charm-quark production in weak charged-current deep-inelastic scattering. The calculation is fully differential based on a generalization of phase-space slicing to NNLO in QCD. The NNLO corrections can change the cross sections by up to 10%, depending on the kinematic region considered. In the kinematic regions of the NuTeV and NOMAD collaborations, our results indicate that once the NNLO corrections are included, the data prefer slightly larger strangeness PDFs in the low-x region than those based on NLO predictions. A definitive result awaits a global analysis with the NNLO corrections included, which is left for future study.

Work at the Argonne National Laboratory (ANL) is supported in part by the U.S. Department of Energy under Contract No. DE-AC02-06CH11357. H. X. Z. was supported by the Office of Nuclear Physics of the U.S. DOE under Contract No. DE-SC0011090. This work was also supported in part by the National Nature Science Foundation of China, under Grants No. 11375013 and No. 11135003. We thank Pavel Nadolsky for his valuable comments and Southern Methodist University for the use of the High Performance Computing facility ManeFrame.

*berger@anl.gov
†jgao@anl.gov
‡csli@pku.edu.cn
§liuzelong@pku.edu.cn
‖zhuhx@mit.edu

[1] P. M. Nadolsky, H.-L. Lai, Q.-H. Cao, J. Huston, J. Pumplin, D. Stump, W.-K. Tung, and C.-P. Yuan, Implications of CTEQ global analysis for collider observables, Phys. Rev. D **78**, 013004 (2008).

[2] A. Kusina, T. Stavreva, S. Berge, F. I. Olness, I. Schienbein, K. Kovařík, T. Ježo, J. Y. Yu, and K. Park, Strange quark PDFs and implications for Drell-Yan boson production at the LHC, Phys. Rev. D **85**, 094028 (2012).

[3] M. W. Krasny, F. Dydak, F. Fayette, W. Placzek, and A. Siodmok, $\Delta M_W \leq 10$ MeV$/c^2$ at the LHC: A forlorn hope?, Eur. Phys. J. C **69**, 379 (2010).

[4] G. Bozzi, J. Rojo, and A. Vicini, Impact of PDF uncertainties on the measurement of the W boson mass at the Tevatron and the LHC, Phys. Rev. D **83**, 113008 (2011).

[5] M. Baak *et al.*, Study of electroweak interactions at the energy frontier, arXiv:1310.6708.

[6] ATLAS Collaboration, Report No. ATL-PHYS-PUB-2014-015, 2014.

[7] F. Carvalho, F. O. Duraes, F. S. Navarra, M. Nielsen, and F. M. Steffens, Meson cloud and SU(3) symmetry breaking in parton distributions, Eur. Phys. J. C **18**, 127 (2000).

[8] R. Vogt, Physics of the nucleon sea quark distributions, Prog. Part. Nucl. Phys. **45**, S105 (2000).

[9] H. Chen, F.-G. Cao, and A. I. Signal, Strange sea distributions of the nucleon, J. Phys. G **37**, 105006 (2010).

[10] M. Goncharov *et al.* (NuTeV Collaboration), Precise measurement of dimuon production cross sections in ν_μ Fe and $\bar{\nu}_\mu$ Fe deep inelastic scattering at the Fermilab Tevatron, Phys. Rev. D **64**, 112006 (2001).

[11] O. Samoylov *et al.* (NOMAD Collaboration), A precision measurement of charm dimuon production in neutrino interactions from the NOMAD experiment, Nucl. Phys. **B876**, 339 (2013).

[12] T. Gottschalk, Chromodynamic corrections to neutrino production of heavy quarks, Phys. Rev. D **23**, 56 (1981).

[13] M. Gluck, S. Kretzer, and E. Reya, Detailed next-to-leading order analysis of deep inelastic neutrino induced charm production off strange sea partons, Phys. Lett. B **398**, 381 (1997); **405**, 392(E) (1997).

[14] J. Blümlein, A. Hasselhuhn, P. Kovacikova, and S. Moch, $O(\alpha_s)$ heavy flavor corrections to charged current deep-inelastic scattering in Mellin space, Phys. Lett. B **700**, 294 (2011).

[15] S. Alekhin, J. Blümlein, L. Caminadac, K. Lipka, K. Lohwasser, S. Moch, R. Petti, and R. Placakyte, Determination of strange sea quark distributions from fixed-target and collider data, Phys. Rev. D **91**, 094002 (2015).

[16] D. A. Mason, Reports No. FERMILAB-THESIS-2006-01 and No. UMI-32-11223, 2006.

[17] A. Kayis-Topaksu *et al.* (CHORUS Collaboration), Leading order analysis of neutrino induced dimuon events in the CHORUS experiment, Nucl. Phys. **B798**, 1 (2008).

[18] B. Pire and L. Szymanowski, Neutrino-Production of a Charmed Meson and the Transverse Spin Structure of the Nucleon, Phys. Rev. Lett. **115**, 092001 (2015).

[19] A. Behring, J. Blümlein, A. De Freitas, A. Hasselhuhn, A. von Manteuffel, and C. Schneider, $O(\alpha_s^3)$ heavy flavor contributions to the charged current structure function $xF_3(x, Q^2)$ at large momentum transfer, Phys. Rev. D **92**, 114005 (2015).

[20] S. Catani and M. H. Seymour, A general algorithm for calculating jet cross sections in NLO QCD, Nucl. Phys. **B485**, 291 (1997); **B510**, 503(E) (1998).

[21] S. Frixione, Z. Kunszt, and A. Signer, Three-jet cross sections to next-to-leading order, Nucl. Phys. **B467**, 399 (1996).

[22] W. T. Giele, E. W. N. Glover, and D. A. Kosower, Higher order corrections to jet cross sections in hadron colliders, Nucl. Phys. **B403**, 633 (1993).

[23] C. Anastasiou, K. Melnikov, and F. Petriello, Higgs Boson Production at Hadron Colliders: Differential Cross Sections through Next-to-Next-to-Leading Order, Phys. Rev. Lett. **93**, 262002 (2004).

[24] A. Gehrmann–De Ridder, T. Gehrmann, and E. W. N. Glover, Antenna subtraction at NNLO, J. High Energy Phys. 09 (2005) 056.

[25] S. Catani and M. Grazzini, Next-to-Next-to-Leading-Order Subtraction Formalism in Hadron Collisions and its Application to Higgs-Boson Production at the Large Hadron Collider, Phys. Rev. Lett. **98**, 222002 (2007).

[26] M. Czakon, A novel subtraction scheme for double-real radiation at NNLO, Phys. Lett. B **693**, 259 (2010).

[27] V. Del Duca, C. Duhr, G. Somogyi, F. Tramontano, and Z. Trócsányi, Higgs boson decay into b-quarks at NNLO accuracy, J. High Energy Phys. 04 (2015) 036.

[28] J. Gaunt, M. Stahlhofen, F. J. Tackmann, and J. R. Walsh, N-jettiness subtractions for NNLO QCD calculations, J. High Energy Phys. 09 (2015) 058.

[29] R. Boughezal, C. Focke, X. Liu, and F. Petriello, W-Boson Production in Association with a Jet at Next-to-Next-to-Leading Order in Perturbative QCD, Phys. Rev. Lett. **115**, 062002 (2015).

[30] J. Gao, C. S. Li, and H. X. Zhu, Top Quark Decay at Next-to-Next-to Leading Order in QCD, Phys. Rev. Lett. **110**, 042001 (2013); A. von Manteuffel, R. M. Schabinger, and H. X. Zhu, The two-loop soft function for heavy quark pair production at future linear colliders, Phys. Rev. D **92**, 045034 (2015); J. Gao and H. X. Zhu, Electroweak production of top-quark pairs in e^+e^- annihilation at NNLO in QCD: The vector contributions, Phys. Rev. D **90**, 114022 (2014); Top-Quark Forward-Backward Asymmetry in e^+e^- Annihilation at Next-to-Next-to-Leading Order in QCD, Phys. Rev. Lett. **113**, 262001 (2014).

[31] I. W. Stewart, F. J. Tackmann, and W. J. Waalewijn, N Jettiness: An Inclusive Event Shape to Veto Jets, Phys. Rev. Lett. **105**, 092002 (2010).

[32] R. Boughezal, J. M. Campbell, R. K. Ellis, C. Focke, W. T. Giele, X. Liu, and F. Petriello, Z-Boson Production in Association with a Jet at Next-to-Next-to-Leading Order in Perturbative QCD, Phys. Rev. Lett. **116**, 152001 (2016).

[33] J. M. Campbell, R. K. Ellis, Y. Li, and C. Williams, Predictions for diphoton production at the LHC through NNLO in QCD, arXiv:1603.02663.

[34] C. F. Berger, C. Marcantonini, I. W. Stewart, F. J. Tackmann, and W. J. Waalewijn, Higgs production with a central jet veto at NNLL + NNLO, J. High Energy Phys. 04 (2011) 092.

[35] C. W. Bauer, S. Fleming, and M. E. Luke, Summing Sudakov logarithms in $B \to X(s\gamma)$ in effective field theory, Phys. Rev. D **63**, 014006 (2000).

[36] C. W. Bauer, S. Fleming, D. Pirjol, and I. W. Stewart, An effective field theory for collinear and soft gluons: Heavy to light decays, Phys. Rev. D **63**, 114020 (2001).
[37] C. W. Bauer, D. Pirjol, and I. W. Stewart, Soft-collinear factorization in effective field theory, Phys. Rev. D **65**, 054022 (2002).
[38] C. W. Bauer, S. Fleming, D. Pirjol, I. Z. Rothstein, and I. W. Stewart, Hard scattering factorization from effective field theory, Phys. Rev. D **66**, 014017 (2002).
[39] I. W. Stewart, F. J. Tackmann, and W. J. Waalewijn, Factorization at the LHC: From PDFs to initial state jets, Phys. Rev. D **81**, 094035 (2010).
[40] E. L. Berger, J. Gao, C. S. Li, Z. L. Liu, and H. X. Zhu (to be published).
[41] R. Bonciani and A. Ferroglia, Two-loop QCD corrections to the heavy-to-light quark decay, J. High Energy Phys. 11 (2008) 065.
[42] H. M. Asatrian, C. Greub, and B. D. Pecjak, Next-to-next-to-leading corrections to $\bar{B} \to X_u \ell \bar{\nu}$ in the shape-function region, Phys. Rev. D **78**, 114028 (2008).
[43] M. Beneke, T. Huber, and X.-Q. Li, Two-loop QCD correction to differential semi-leptonic $b \to u$ decays in the shape-function region, Nucl. Phys. **B811**, 77 (2009).
[44] G. Bell, NNLO corrections to inclusive semileptonic B decays in the shape-function region, Nucl. Phys. **B812**, 264 (2009).
[45] T. Becher and M. Neubert, Toward a NNLO calculation of the $\bar{B} \to X_s \gamma$ decay rate with a cut on photon energy: I. Two-loop result for the soft function, Phys. Lett. B **633**, 739 (2006).
[46] J. R. Gaunt, M. Stahlhofen, and F. J. Tackmann, The quark beam function at two loops, J. High Energy Phys. 04 (2014) 113.
[47] J. M. Campbell and F. Tramontano, Next-to-leading order corrections to Wt production and decay, Nucl. Phys. **B726**, 109 (2005).
[48] G. Cullen *et al.*, GOSAM2.0: a tool for automated one-loop calculations within the Standard Model and beyond, Eur. Phys. J. C **74**, 3001 (2014).
[49] H. Murayama, I. Watanabe, and K. Hagiwara, Report No. KEK-91-11, 1992.
[50] S. Catani, S. Dittmaier, M. H. Seymour, and Z. Trocsanyi, The dipole formalism for next-to-leading order QCD calculations with massive partons, Nucl. Phys. **B627**, 189 (2002).
[51] S. Dulat, T.-J. Hou, J. Gao, M. Guzzi, J. Huston, P. Nadolsky, J. Pumplin, C. Schmidt, D. Stump, and C.-P. Yuan, New parton distribution functions from a global analysis of quantum chromodynamics, Phys. Rev. D **93**, 033006 (2016).
[52] J. Beringer *et al.* (Particle Data Group Collaboration), Review of Particle Physics, Phys. Rev. D **86**, 010001 (2012).
[53] Throughout this Letter, we do not include higher-twist effects, nuclear corrections, electroweak corrections, or target-mass corrections. They should be considered when making a comparison to experimental data, and they can be applied separately from the perturbative QCD corrections shown here.
[54] M. Brucherseifer, F. Caola, and K. Melnikov, On the NNLO QCD corrections to single-top production at the LHC, Phys. Lett. B **736**, 58 (2014).
[55] S. Alekhin, J. Blumlein, and S. Moch, OPENQCDRAD, https://www-zeuthen.desy.de/~alekhin/OPENQCDRAD/.
[56] J. Blümlein, A. Hasselhuhn, and T. Pfoh, The $O(\alpha_s^2)$ heavy quark corrections to charged current deep-inelastic scattering at large virtualities, Nucl. Phys. **B881**, 1 (2014).